Korean J. Chem. Eng., 38(9), 1781-1790 (2021)
DOI: 10.1007/s11814-021-0822-4

pISSN: 0256-1115
eISSN: 1975-7220

Prediction of gas holdup in various types of airlift reactors

Keun Ho Choi†

Department of Chemical and Biological Engineering, Hanbat National University,
125, Dongseodaero, Yoseong-gu, Daejeon 305719, Korea
(*Received 15 February 2021 • Revised 5 April 2021 • Accepted 23 April 2021*)

Abstract−Useful correlations were derived for the prediction of available gas holdup data in air-water systems, using the operational and geometric parameters of airlift reactors only. To successfully consider the geometric difference between various types of airlift reactors, the characteristic distance (D_{ch}) and the gas separation area (A_s) were defined as geometric parameters, respectively. The riser gas holdup (ε_r) in various types of airlift reactors was satisfactorily correlated with the operational and geometric parameters, such as the riser superficial gas velocity (U_{Gr}), a parameter containing the ratio of the top clearance to downcomer length ($1+C_t/L_d$), the characteristic distance to downcomer length ratio (D_{ch}/L_d), the downcomer to riser cross-sectional area ratio (A_d/A_r), the ratio of the gas separation area to riser cross-sectional area (A_s/A_r), and the bottom to downcomer cross-sectional area ratio (A_b/A_d). The downcomer gas holdup in various types of airlift reactors was well correlated by a nonlinear equation involving ε_r, D_{ch}/L_d, A_d/A_r, A_b/A_d, $(1+C_t/L_d)$, and A_s/A_r.

Keywords: Prediction, Gas Holdup, Airlift Reactor, Characteristic Distance, Gas Separation Area

INTRODUCTION

Airlift reactors can be clearly classified into two large groups: external-loops and internal-loops [1-3]. External-loop airlift reactors have two separate and vertical pipes that are joined by the top and bottom connections. Sometimes the connections are horizontal pipes. Gas-liquid separation takes place in the top region of the airlift reactors including the top connection pipe. A rectangular tank is frequently used as the top connection in order to increase its mixing performance and gas-liquid separation efficiency. Accordingly, the rectangular tank is especially called a gas-liquid separator. One of these vertical pipes is the riser, which has an upward flow of fluid. The other pipe is the downcomer, which has a downward flow of fluid. Internal-loop airlift reactors are characterized by having a vessel that is divided by a vertical baffle or a draft-tube. The cross-section of the vessel is usually circular, sometimes rectangular [4]. The top and the bottom of the vessel take roles of the top and the bottom connection for external-loop airlift reactors, respectively.

Many researchers have investigated a large number of modified airlift reactors: the riser with various internals (baffles [5,6], perforated plates [7-10], disks [11], static mixers [12-14], impellers [15, 16], packing materials [17]), multiple draft tubes [18,19], the enlarged top [20-24], inclined connection pipes [14,25-28], the downcomer without an extension tube [29-33], multi-stages [34,35], the top with funnel internals [36], and net draft tubes [37]. Therefore, there are many types of airlift reactors. Different morphologies of airlift reactors result in very different trends of performance factors such as gas holdup, mixing time, circulation liquid velocity, and oxygen transfer coefficient.

All researchers observed that the riser and downcomer gas holdups increase with the riser superficial gas velocity (U_{Gr}). Bello et al. [38] expressed the gas holdup as a function of specific power input instead of the gas velocity. The influence of the bottom and top clearances on the gas holdup was studied by Koide et al. [39], Merchuk et al. [22], Choi [40], and Gouveia et al. [41]. A large number of published works on airlift reactors have focused on the effect of the downcomer to riser cross-sectional area ratio (A_d/A_r) [4,42-50]. There are some correlations on the gas holdups as a function of the superficial liquid velocity (U_{Lr}) [44,51-55]. The length of the connection pipe or the distance between the riser and downcomer axes has also a strong effect on the gas holdup [47,48,56]. Zhao et al. [8], Rujiruttanakul and Pavasant [28], Kojić et al. [57], and Luo et al. [58] reported that the sparger structure had a significant effect on the gas holdup and downcomer liquid velocity. Some researchers studied the effect of liquid properties such as viscosity and density on the gas holdup [39,42,45,46,53,55, 57,59,60].

Up to now, many correlations for gas holdup in airlift reactors have been reported in the literature. However, most of the correlations are only useful for a particular type of airlift reactor from which they were derived. The gas holdup data obtained in the other type of airlift reactors differed greatly from the correlations. Therefore, the previous correlations for gas holdup are extremely limited in use.

If we obtain a correlation equation that can well predict a large amount of the gas holdup obtained in various types of airlift reactors, we can use it more usefully than previous correlations for reactor design. Therefore, in this work, new geometric parameters such as the characteristic distance (D_{ch}) and the gas separation area (A_s) were defined and used to reflect the effect of reactors' geometrical difference on the gas holdup. We attempted to correlate as many gas holdup data obtained in four basic types of airlift reactors and

†To whom correspondence should be addressed.
E-mail: khchoi@hanbat.ac.kr

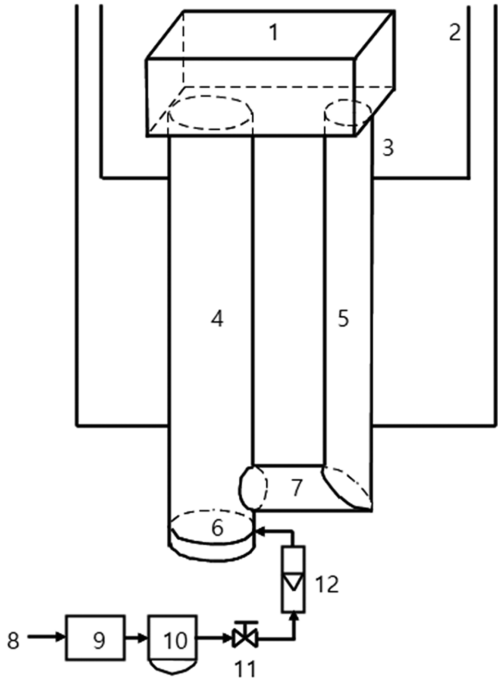

Fig. 1. Schematic diagram of the experimental apparatus.

1. Gas-liquid separator	7. Bottom connection pipe
2. Pressure tap	8. Air line
3. Piezometer tube	9. Air filter
4. Riser	10. Pressure regulator
5. Downcomer	11. Valve
6. Gas sparger	12. Rotameter

air-water systems as possible with the operational and geometric parameters only. The operational parameters were the riser superficial gas velocity (U_{Gr}) and a parameter containing the ratio of top clearance to downcomer length ($1+C_t/L_d$). The geometric parameters were ratios between the free areas of conduits for circulation liquid [i.e., the downcomer to riser cross-sectional area ratio (A_d/A_r), the bottom to downcomer cross-sectional area ratio (A_b/A_d)] as well as the ratio of the characteristic distance to the downcomer length (D_{ch}/L_d) and the ratio of the gas separation area to riser area (A_s/A_r).

EXPERIMENTAL

The external-loop airlift reactor used in this work had a gas-liquid separator as shown in Fig. 1. The inside diameter of the riser was 0.149 m. Its height was 1.782 m. The inside diameter of the downcomer was 0.108 m. The connection pipe joined the downcomer to the riser 0.10 m above the bottom plate. The length of the connection pipe was 0.30 m. The upper tips of the riser and the downcomer were attached to the gas-liquid separator (0.70×0.26×0.30 m). A set of six tubes (outside diameter 6 mm) welded on the bottom plate was used as a gas sparger. Each tube had several holes (inside diameter 1 mm). A total of 30 holes was arranged in a triangular pitch of 21 mm [56]. The velocity of air input was measured with a calibrated rotameter. Riser superficial gas velocity was varied in the range of 0.02 to 0.18 m s^{-1}. All experimental measurements were performed at atmospheric pressure and room temperature (22.5-25.5 °C).

For gas holdup measurements by differential hydrostatic pressure method, two piezometer tubes were installed on the riser and the downcomer, respectively. The heights of the pressure taps were 0.40 and 1.50 m from the bottom plate. To decrease the variation of piezometer reading, a capillary tube of length 7 mm and inside diameter 0.7 mm was inserted at the entrance of the piezometer tubes [61,62]. A video of the readings of the piezometer tubes was taken by a cellular phone (LG G Flex) a minute at a specific gas flow rate. Freeze-frames extracted every second from the video were used to calculate the riser and downcomer gas holdups [63]. Therefore, each gas holdup was an average of 61 measurements. The gas holdups were calculated from the following equation:

$$\varepsilon = \frac{\rho_L}{\rho_L - \rho_G}\frac{\Delta h}{\Delta Z} \tag{1}$$

RESULTS AND DISCUSSION

Main correlations for the riser and downcomer gas holdups (ε_r and ε_d) in various types of airlift reactors are summarized in Table 1. Gas holdup data used for obtaining useful correlations in this study are shown in Table 2. As shown in Tables 1 and 2, many researchers performed measurements of the riser and downcomer

Table 1. Correlations for gas holdup in various types of airlift reactors

Authors	Type*	Proposed correlations
Chakravarty et al. [42]	DTIL	$\varepsilon_r = \left\{(\mu_L - \mu_W)^{2.75} + 161\left(\frac{73.3-\sigma_L}{74.1-\sigma_L}\right)\right\} \times 10^{-4} U_{Gr}^{0.88}$
Hills [51]	ELGS	$\varepsilon_r = \frac{U_{Gr}}{0.24 + 1.35(U_{Gr}+U_{Lr})^{0.093}}$
Merchuk and Stein [52]	ELGS	$\varepsilon_r = \frac{U_{Gr}}{0.33 + 1.03(U_{Gr}+U_{Lr})}$
Bello et al. [64]	ELET DTIL	$\varepsilon_r = 0.16\left(\frac{U_{Gr}}{U_{Lr}}\right)^{0.56}\left(1+\frac{A_d}{A_r}\right)$ ELET: $\varepsilon_d = 0.79\varepsilon_r - 0.057$ DTIL: $\varepsilon_d = 0.89\varepsilon_r$

Table 1. Continued

Authors	Type*	Proposed correlations
Bello et al. [38]	ELET	$\varepsilon_r = 3.4\times10^{-3}\left(1+\frac{A_d}{A_r}\right)^{-1}\left(\frac{P_G}{V_D}\right)^{2/3}$
Chisti et al. [43]	RIL	bubble flow: $\varepsilon_r = (1.488-0.496C_s)\left(\frac{U_{Gr}}{1+A_d/A_r}\right)^{0.892\pm0.075}$ coalesced bubble flow: $\varepsilon_r = (0.371-0.089C_s)\left(\frac{U_{Gr}}{1+A_d/A_r}\right)^{0.430\pm0.015}$
	ELET	$\varepsilon_r = 0.65\left(1+\frac{A_d}{A_r}\right)^{-0.258}U_{Gr}^{0.603\pm0.078C_s}$
Miyahara et al. [53]	DTIL	$\varepsilon_r = \frac{0.4\sqrt{F_r'}}{1+0.4\sqrt{F_r'}(1+U_{Lr}/U_{Gr})}$ $\varepsilon_d = 4.51\times10^6 M^{0.115}\left(\frac{A_r}{A_d}\right)^{4.2}\varepsilon_r^{4.2}$ for $\varepsilon_d<0.0133\left(\frac{A_r}{A_d}\right)^{-1.32}$ $\varepsilon_d = 0.55M^{-0.22}\left\{\left(\frac{A_r}{A_d}\right)^{0.6}\varepsilon_r\right\}^{0.31M^{-0.073}}$ for $\varepsilon_d>0.0133\left(\frac{A_r}{A_d}\right)^{-1.32}$
Popović and Robinson [46]	ELET	$\varepsilon_r = 0.465U_{Gr}^{0.650}\left(1+\frac{A_d}{A_r}\right)^{-1.06}\mu_{eff}^{-0.103}$
Choi et al. [56]	ELET	$\varepsilon_r = 0.43U_{Gr}^{0.65}\left(\frac{L_c}{L_{co}}\right)^{-0.15}$ $\varepsilon_d = 0.09U_{Gr}^{1.01}\left(\frac{L_c}{L_{co}}\right)^{-0.92}$
Philip et al. [54]	DTIL	$\varepsilon_r = \frac{U_{Gr}}{C_1(U_{Gr}+U_{Lr})+C_2\sqrt{gD_c}}$ where $C_1=\frac{3n+1}{n+1}$ C_2=0.24-0.33 for Newtonian flow C_2=0.35 for Non-Newtonian flow
Choi and Lee [47]	ELET	$\varepsilon_r = 0.288U_{Gr}^{0.504}\left(\frac{A_d}{A_r}\right)^{-0.098}\left(\frac{L_c}{L_h}\right)^{-0.094}$ $\varepsilon_d = 0.049U_{Gr}^{1.138}\left(\frac{A_d}{A_r}\right)^{-0.885}\left(\frac{L_c}{L_h}\right)^{-0.462}$
Kemblowski et al. [55]	ELGS	$\varepsilon_r = 0.203\frac{\left[\frac{U_{Gr}+U_{Lr}}{gD_r}\right]^{0.31}}{\left[\frac{g(\rho_L-\rho_G)k^4}{\sigma_L^3\rho_L^2}\left(\frac{8U_{Lr}}{D_r}\right)^{4(n-1)}\left(\frac{3n+1}{4n}\right)^{4n}\right]^{0.012}\left(\frac{U_{Gr}A_r}{U_{Lr}A_d}\right)^{0.57}}$
Merchuk et al. [22]	DTIL	$\varepsilon_r = 1.5\left(\frac{U_{Gc}}{\sqrt{gD_c}}\right)^{0.87}\left(\frac{D_s}{4D_c}\right)^{-0.04}\left(\frac{C_b}{D_c}\right)^{-0.19}\left(\frac{C_t}{D_d}\right)^{-0.2}$ $\varepsilon_d = 4.76\left(\frac{U_{Gc}}{\sqrt{gD_c}}\right)^{1.3}\left(\frac{D_s}{4D_c}\right)^{-3.8}\left(\frac{C_b}{D_c}\right)^{-0.65}\left(\frac{\rho_L^2D_c^3C_t}{\mu^2}\right)^{-0.09}$
Bentifraouine et al. [65]	ELET ELGS	$\varepsilon_r = 2U_{Gr}^{0.88}(1-0.97U_{Lr}^{0.49})$
Couvert et al. [66]	SRIL	$\varepsilon_r = 0.137U_{Gr}^{0.92}$
Lu et al. [4]	DTIL	$\varepsilon_r = 0.035U_{Gr}^{0.647}\left(\frac{A_d}{A_r}\right)^{-0.085}$
Choi [48]	ELCD	$\varepsilon_r = 0.431U_{Gr}^{0.580}\left(\frac{A_d}{A_r}\right)^{-0.040}\left(\frac{L_c}{L_h}\right)^{-0.042}$

Table 1. Continued

Authors	Type*	Proposed correlations
Choi [49]	ELGS	$\varepsilon_r=0.2447U_{Gr}^{0.5616}\left(\frac{A_d}{A_r}\right)^{-0.2779}C_t^{-0.0130}$
Gouveia et al. [41]	DTIL	$\varepsilon_r=11.97\left(\frac{U_{Gr}}{\sqrt{gD_r}}\right)^{1.31}\left(\frac{C_b}{D_r}\right)^{0.42}\left(\frac{C_t}{D_r}+1\right)^{-2.44}$ $\varepsilon_d=13.52\left(\frac{U_{Gr}}{\sqrt{gD_r}}\right)^{1.46}\left(\frac{C_b}{D_r}\right)^{0.72}\left(\frac{C_t}{D_r}+1\right)^{-5.21}$
Al-Masry [67]	ELGS	$\varepsilon_r=3.84[(0.73U_{Gr}+1)^{1.33}-1]^{1/1.33}\times\exp\left[-0.0067T_{VR}-1.095\left(\frac{A_d+A_r}{A_r}\right)+0.084\mu_L\right]$ $\varepsilon_d=2.69[(0.47U_{Gr}+1)^{1.29}-1]^{1/1.29}\times\exp\left[-0.011T_{VR}-0.69\left(\frac{A_d+A_r}{A_r}\right)+0.075\mu_L\right]$
Yazdian et al. [50]	ELCD	$\varepsilon_r=13.19U_{Gr}^{1.43}\left(1+\frac{A_r}{A_d}\right)^{-0.62}(1+S)^{-0.58}\left(\frac{\nu_g}{\nu_{N_2}}\right)^{-0.52}$ $\varepsilon_r=0.47\varepsilon_d$
Rujiruttanakul and Pavasant [28]	ELET	$\varepsilon_r=0.49U_{Gr}^{0.67}L_c^{-0.15}L_h^{-0.22}$ $\varepsilon_d=0.29U_{Gr}L_c^{-0.45}L_h^{0.39}$
Kojić et al. [57]	ELGS	$\varepsilon_r=2.35U_{Gr}^{0.66}\sigma^{-0.47}\phi^{-0.045}\left(\frac{A_d}{A_r}\right)^{-0.61}$

*DTIL, draft-tube internal-loop; ELCD, external-loop with a closed downcomer; ELET, external-loop with an extension tube; ELGS, external-loop with a gas-liquid separator; RIL, rectangular internal-loop; SRIL, split rectangular internal-loop.

gas holdups in four basic types of airlift reactors, such as draft-tube internal-loop (DTIL), split rectangular internal-loop (SRIL), external-loop with an extension tube (ELET), and external-loop with a gas-liquid separator (ELGS). Previous investigations show that the gas holdup depends on the operational and geometric parameters of the reactors. The operational parameters are superficial gas velocity, superficial liquid velocity, top clearance (or liquid volume), and properties of liquids. The main construction parameters of airlift reactors are the downcomer to riser cross-sectional area ratio (A_d/A_r), the bottom clearance, the connection pipe to downcomer length ratio (D_c/L_d), design of the gas sparger, and details of the gas-liquid separator.

The main parameters that influence the riser gas holdup in various types of airlift reactors must be taken into account in order to achieve a meaningful correlation of the results. However, the riser superficial liquid velocity, design of the gas sparger, and properties of the liquid (for instance, viscosity, surface tension, and ionic concentration) were not considered because of two reasons: first, their effect on gas holdup was not experimented in this study; second, there is still not enough research literature on their effect on gas holdup in airlift reactors.

In this work, in order to successfully correlate as many gas holdup data as possible, the characteristic distance (D_{ch}) and the gas separation area (A_s) for each type of airlift reactors were defined and were used as geometric parameters. The characteristic distance was defined as follows:

$$D_{ch}=\frac{D_d+D_c}{4} \quad \text{for DTIL} \tag{2}$$

$$D_{ch}=\frac{W_r+W_d}{2} \quad \text{for SRIL} \tag{3}$$

$$D_{ch}=\frac{D_r}{2}+\frac{D_d}{2}+L_c \quad \text{for ELET and ELGS} \tag{4}$$

If air bubbles released from the riser do not separate from the gas-liquid mixture in the top region including the top connection pipe, they flow into the downcomer by liquid circulation. Most large bubbles are separated just after the time when the circulation liquid changes its direction to the downcomer. After that, when the circulation liquid flows through the horizontal conduits such as the top connection pipe and the gas-liquid separator, small bubbles continuously go up the liquid surface due to buoyancy force and effectively escape from the liquid because the liquid height in the conduits is low. The longer the horizontal distance which bubbles travel from the riser to the downcomer, the fewer bubbles are entrained into the downcomer. In general, the horizontal distance for internal-loop airlift reactors is smaller than that for external-loop airlift reactors. In addition, it is certain that the longer the residence time of the circulation liquid in the top region, the smaller the downcomer gas holdup is. Considering the phenomenon, the gas separation area (A_s) was defined as the largest cross-sectional area of the top region in Fig. 2. For external-loop airlift reactors

Table 2. Used gas holdup data for obtaining the correlations

No.	Authors	Type	Conditions	Used data
1	Chakravarty et al. [42]	DTIL	D_c=0.1 m, D_d=0.059 m, L_d=0.4, C_b=0.026 m, C_t=0.06 m, V_L=3.8×10^{-2} m^3, perforated plate sparger (ϕ=1.5 mm)	ε_r, ε_d
2	Jones [68]	DTIL	D_c=0.25 m, D_d=0.044-0.146 m, L_d=1.22 m, C_b=0.1 m, C_t=0.01 m, tube sparger (ϕ=2.4 mm)	ε_r
3	Choi et al. [7]	DTIL	D_c=0.238 m, D_d=0.146 m, L_d=0.992 m, t_d=0.006 m, H_d=1.55 m, C_b=0.05 m, tube sparger (ϕ=1 mm)	ε_r, ε_d
4	Miyahara et al. [53]	DTIL	D_c=0.148 m, D_d=0.07 m, L_d=1.0 m, t_d=0.005 m, C_b=0.08 m, C_t=0.06 m, perforated plate sparger (ϕ=1 mm)	ε_r
5	Wachi et al. [69]	DTIL	D_c=0.22 m, D_d=0.12 m, L_d=1.95 m, U_{Gr}=0.02-0.07 m, t_d=0.005 m, C_b=0.05 m, V_L=8.5×10^{-2} m^3, perforated plate sparger (ϕ=0.5 mm)	ε_r, ε_d
6	Petrović et al. [70]	DTIL	D_c=0.20 m, D_d=0.08-0.15 m, L_d=2 m, t_d=0.006 m, C_b=0.040 m, perforated plate sparger (ϕ=1 mm)	ε_r, ε_d
7	Merchuk et al. [22]	DTIL	D_c=0.318 m, D_d=0.216 m, L_d=3.27 m, t_d=0.041 m, C_b=0.01-0.08 m, C_t=0.04 m, V_L=3.00×10^{-1} m^3, ring sparger (ϕ=1 mm)	ε_r, ε_d
		DTIL	D_c=0.158 m, D_d=0.110 m, L_d=1.395 m, D_s=0.213 m, C_b=0.012 m, C_t=0.308 m, V_L=3.0×10^{-2} m^3, ring sparger (ϕ=1 mm)	ε_d
8	Lu et al. [71]	DTIL	D_c=0.18 m, D_d=0.12 m, L_d=1.10 m, t_b=0.005 m, C_b=0.10 m, C_t=0.20 m, U_{Gr}=0.015-0.147 m s^{-1}, ring sparger	ε_r, ε_d
9	Blažey et al. [24]	DTIL	D_c=0.147 m, D_d=0.106 m, L_d=1.71 m, t_d=0.006 m, H_L=1.818 m, D_s=0.294 m, C_b=0.046 m, C_t=0.062 m, V_L=3.2×10^{-2} m^3, perforated plate sparger	ε_r, ε_d
10	Blažey et al. [72]	DTIL	D_c=0.294 m, D_d=0.200 m, L_d=2.7 m, H_L=2.936 m, C_b=0.061 m, C_t=0.175 m, V_L=2.00×10^{-1} m^3, perforated plate sparger	ε_r, ε_d
11	Siegel et al. [61]	SRIL	W_r=0.07 m, W_d=0.09 m, W_c=0.25 m, L_d=4.0 m, C_b=C_t=0.10 m, L_s×W_s×H_s=0.32×0.25×0.64 m, ϕ=0.5-2.5 mm, straight baffle	ε_r
12	Couvert et al. [66]	SRIL	W_r=W_d=0.25 m, W_c=0.5 m, L_d=2.35 m, C_b=0.15 m, C_t=0.1 m, U_{Gr}=0.011-0.045 m s^{-1}, tubular plastic membranes	ε_r, ε_d
13	Popović and Robinson [73]	ELET	D_r=0.15 m, D_d=0.05 m, L_d=1.78 m, L_c=0.432 m, C_t=0 m**, perforated plate sparger (ϕ=1 mm)	ε_r
14	Choi and Lee [47]	ELET	D_r=0.149 m, D_d=0.049-0.108 m, L_d=0.992 m, L_c=0.10-0.50 m, H_d=1.77 m, U_{Gr}=0.02-0.18 m s^{-1}, tube sparger (ϕ=1 mm)	ε_r, ε_d
15	Al-Masry and Dukkan [74]	ELET	D_r=D_d=0.225 m, L_d=7.5 m, L_c=1.2 m, V_L=0.7 m^3, plate sparger	ε_r, ε_d
16	Bentifraouine et al. [75]	ELET	D_r=0.194 m, D_d=0.92 m, L_d=0.908 m, H=1.40 m, D_{ch}=0.50 m, C_t=0 m**, ring sparger (ϕ=0.8 mm)	ε_r
17	Rujiruttanakul and Pavasant [28]	ELET	D_r=0.104 m, D_d=0.054 m, L_d=1.346 m, L_c=0.2 m, C_t=0.03 m, H_L=1.56 m, porous plate sparger	ε_r, ε_d
18	Kemblowski et al. [55]	ELGS	D_r=D_d=0.100 m, L_d=1.800 m, L_c=0.40 m**, H_d=1.77 m, U_{Gr}=0.015-0.09 m s^{-1}, L_s×W_s×H_s=1.00×0.30×0.30 m, porous plate sparger	ε_r
19	Bentifraouine et al. [65]	ELGS	D_r=0.194 m, D_d=0.093 m, H=1.60 m, D_{ch}=0.50 m, tube sparger (ϕ=0.6 mm)	ε_r
20	Choi [40]	ELGS	D_r=0.149 m, D_d=0.049-0.108 m, L_d=1.578 m, L_c=0.3 m, C_t=0-0.20 m, U_{Gr}=0.20-0.18 m s^{-1}, L_s×W_s×H_s=0.70×0.26×0.30 m, tube sparger (ϕ=1 mm)	ε_r
21	This work	ELGS	D_r=0.149 m, D_d=0.108 m, L_d=1.578 m, L_c=0.3 m, C_t=0 m, U_{Gr}=0.02-0.18 m s^{-1}, L_s×W_s×H_s=0.70×0.26×0.30 m, tube sparger (ϕ=1 mm)	ε_r, ε_d

**Assumed value

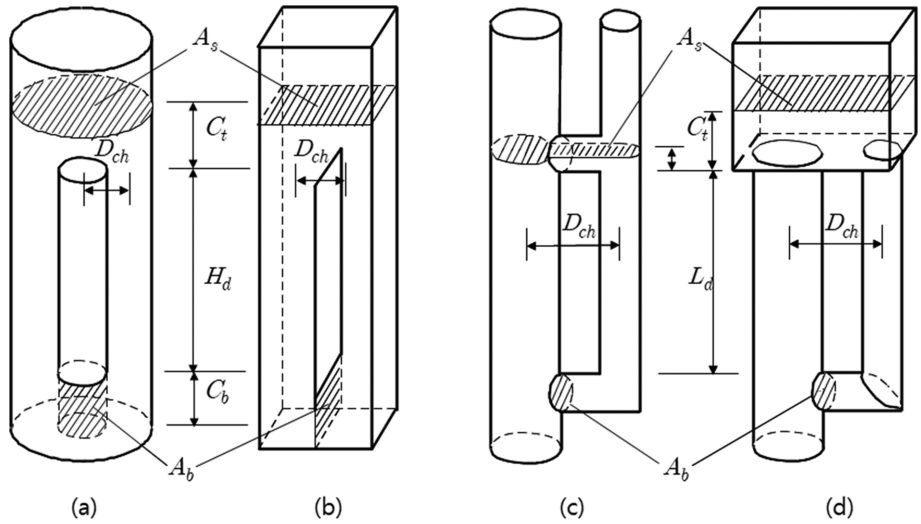

Fig. 2. Definitions of cross-sectional areas and dimensions: (a) Draft-tube internal-loop; (b) split rectangular internal-loop; (c) external-loop with an extended tube; (d) external-loop with a gas-liquid separator.

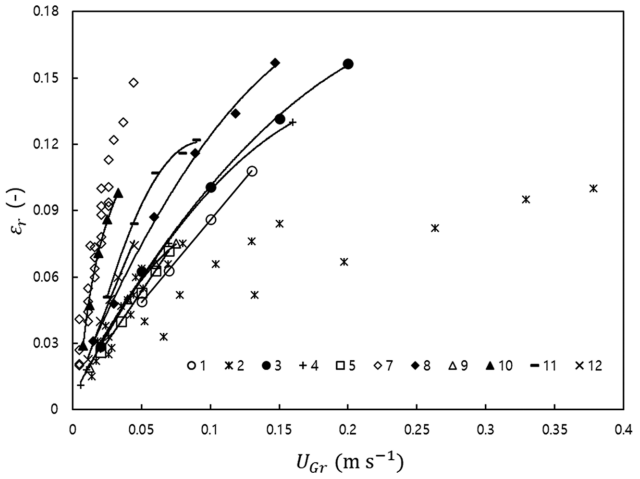

Fig. 3. Riser gas holdup in internal-loop airlift reactors. See Table 2 for legend.

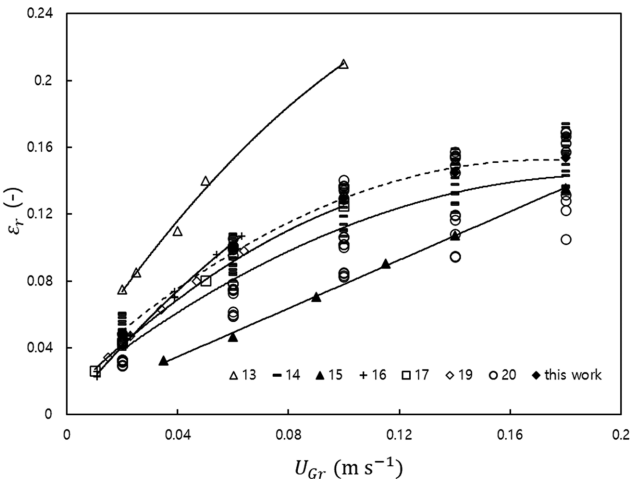

Fig. 4. Riser gas holdup in external-loop airlift reactors. See Table 2 for legend.

with the extension tube, it was the sum of the cross-sectional areas of the riser, the downcomer, and the top connection pipe.

To predict liquid circulation velocity, Chisti et al. [76] defined the bottom clearance area (A_b) between the riser and the downcomer (the hatched area in Fig. 2). In this work, considering the effect of the bottom clearance on the gas holdup, the bottom clearance area was used as a geometric parameter. Finally, the selected parameters for the prediction of gas holdup in various types of airlift reactors were the riser superficial gas velocity (U_{Gr}), a parameter containing the ratio of the top clearance to downcomer length ($1+C_t/L_d$), the characteristic distance to downcomer length ratio (D_{ch}/L_d), the downcomer to riser cross-sectional area ratio (A_d/A_r), the ratio of the gas separation area to riser cross-sectional area (A_s/A_r), and the bottom to downcomer cross-sectional area ratio (A_b/A_d).

Available riser gas holdup data for the internal-loop and external-loop airlift reactors in the literature are presented in Figs. 3 and 4, respectively. The dotted line in Fig. 4 represents my data measured in this work, while the solid lines in Figs. 3 and 4 represent a selected part of the data to show the trends of the riser gas holdup as a function of the riser superficial gas velocity. The riser gas holdup increased with increasing superficial gas velocity. At low gas velocities, the riser gas holdup increased sharply, while at high gas velocities it became constant. Most of the reported data on gas holdup in the riser differentiated between the geometrical differences of the reactors. Regardless of the internal-loop and external-loop airlift reactors, at a given value of the superficial gas velocity, the riser gas holdup could differ from reactor to reactor up to about four times.

A correlation involving U_{Gr} and dimensionless form of parameters, such as D_{ch}/L_d, A_d/A_r, A_b/A_d, A_s/A_r, $(1+C_t/L_d)$, was used to describe the variations of the riser gas holdup in the reactors. The results are plotted in Fig. 5. The riser gas holdup in the literature and my data in air-water systems are well represented by Eq. (5), with a respective correlation coefficient of 0.91. Eq. (5) fits 288 data with

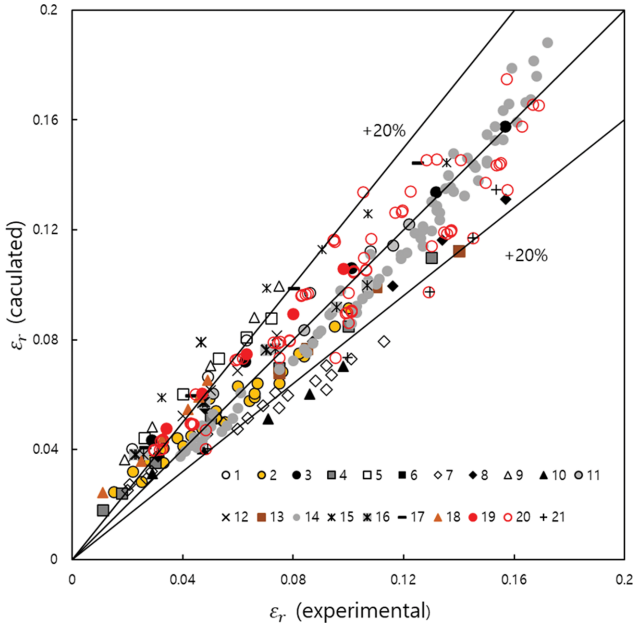

Fig. 5. Comparison between calculated and experimental results of riser gas holdup in various types of airlift reactors.

the mean absolute percentage error of 16.5%.

$$\varepsilon_r = 0.322\left(\frac{D_{ch}}{L_d}\right)^{-0.16}\left(\frac{A_d}{A_r}\right)^{-0.235}\left(\frac{A_b}{A_d}\right)^{-0.119}\left(1+\frac{C_t}{L_d}\right)^{-0.119}\left(\frac{A_s}{A_r}\right)^{-0.129} U_{Gr}^{0.548} \quad (5)$$

The ranges of the parameters are $0.02 \le D_{ch}/L_d \le 0.638$, $0.108 \le A_d/A_r \le 30.99$, $0.170 \le A_b/A_d \le 4.858$, $1 \le (1+C_t/L_d) \le 1.384$, $2 \le A_s/A_r \le 38.217$, and $0.005\ m\ s^{-1} \le U_{Gr} \le 0.37\ m\ s^{-1}$. As shown in Table 1, the data of most authors show that the range of the exponent for U_{Gr} is between 0.415 [43] and 1.43 [50]. The exponent for U_{Gr} in Eq. (5) is slightly lower than 0.56 obtained by Bello et al. [64]. Choi [49] reported that the exponent for U_{Gr} was 0.5616.

A wide range of experimental conditions and various reactor configurations were considered in this work. As seen in Fig. 5, Eq. (5) is a useful means for predicting the riser gas holdup. The data in Fig. 5 represent 42 different airlift reactors covering approximately 32-fold variation in D_{ch}/L_d, about 287-fold variation in A_d/A_r, around 29-fold variation in A_b/A_d, approximately 1.4-fold variation in $(1+C_t/L_d)$ and around 19-fold variation in A_s/A_r. These broad ranges demonstrate the applicability of Eq. (5) for airlift reactor design. Many conditions that show a larger deviation over ±30% than the calculated value by Eq. (5) are low gas velocity ($0.07\ m\ s^{-1} < U_{Gr}$). Of those, the measured gas holdup of Blazey et al. [24] on average is 53% lower than predicted by Eq. (5). This difference can be attributed to the high liquid velocity, caused by the enlarged top in their case. The data of Kemblowski et al. [55] also show relatively a large deviation. It may be due to the assumed value of L_c.

As previously pointed out, the top region in external-loop airlift reactors can be an effective gas-liquid separator that ensures the disengagement of most air bubbles from the liquid before they enter the downcomer. Therefore, the literature on the downcomer gas holdup is relatively scant. The available downcomer gas holdup for various types of airlift reactors in the literature, together with

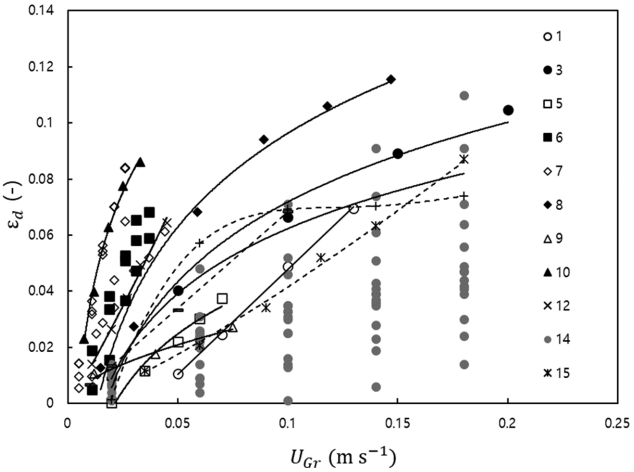

Fig. 6. Downcomer gas holdup in various types of airlift reactors. See Table 2 for legend.

my results, are shown in Fig. 6. The solid lines represent a selected part of the data for the internal-loop airlift reactors, whereas the dotted lines represent a selected part of the data for the external-loop airlift reactors. In general, at a specific gas velocity, the downcomer gas holdup for the external-loop airlift reactors is smaller than that of the internal-loop airlift reactors because of increasing circulation liquid velocity. Many researchers reported that the downcomer gas holdup was increased with increasing circulation liquid velocity. In addition, at the same value of the superficial gas velocity, the downcomer gas holdup could very much differ from reactor to reactor because of the difference between the gas-liquid separation efficiency of the top regions. The top region of the airlift reactor can be designed for complete gas-liquid separation [77].

Empirical linear relationships between the downcomer and riser gas holdups were proposed by some researchers [44,50,78,79]:

$$\varepsilon_d = a\varepsilon_r + b \quad (6)$$

where a and b were constants. Bello et al. [44] reported that b was

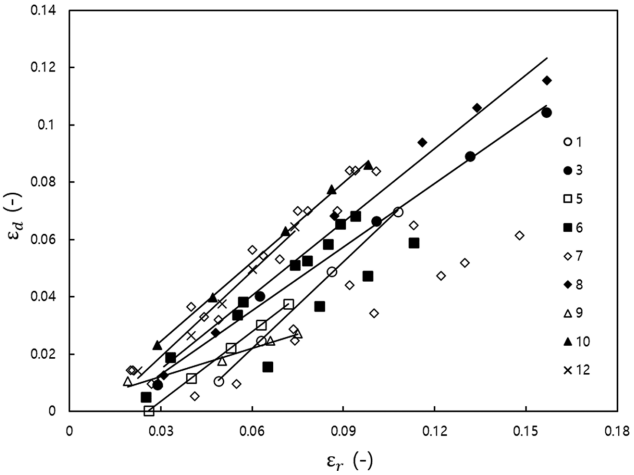

Fig. 7. Relationships between riser gas holdup and downcomer gas holdup in internal-loop airlift reactors. See Table 2 for legend.

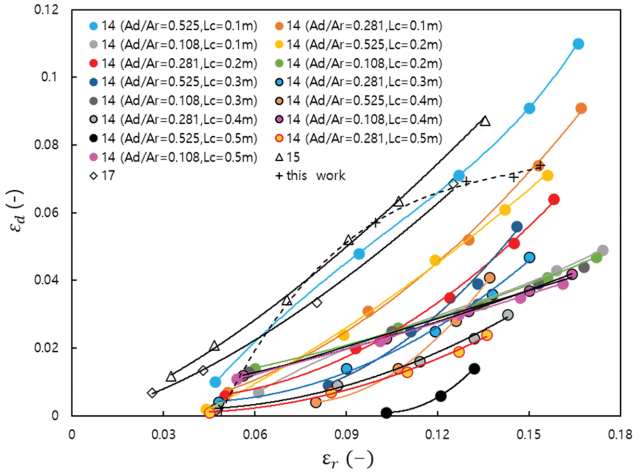

Fig. 8. Relationships between riser gas holdup and downcomer gas holdup in external-loop airlift reactors. See Table 2 for legend.

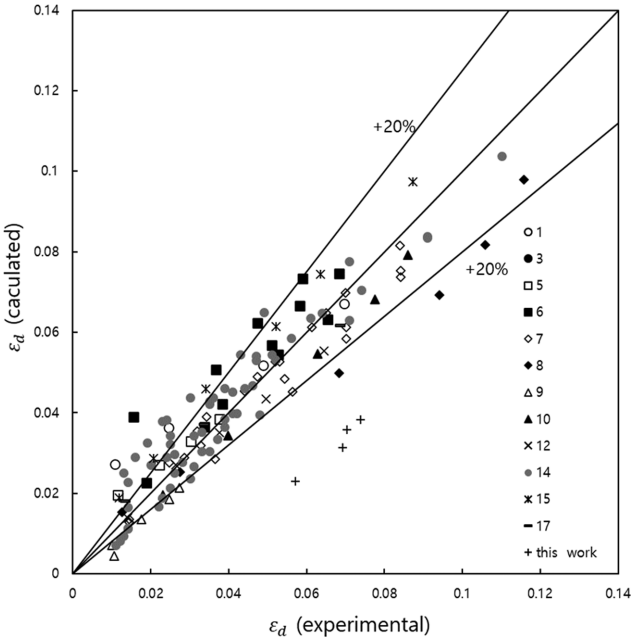

Fig. 9. Parity plot of downcomer gas holdup correlation, Eq. (7), for various types of airlift reactors. See Table 2 for legend.

equal to 0 for the draft-tube airlift reactors. However, as shown in Fig. 7, it is certain that the dependency of the constants in Eq. (6) on geometric parameters is very complex even in the case of internal-loop airlift reactors. Furthermore, for external-loop airlift reactors, the relationship between the riser and downcomer gas holdups is nonlinear as Fig. 8 shows. Miyahara et al. [53] also obtained a nonlinear relationship for the draft-tube airlift reactors as shown in Table 1. My own data in the external-loop airlift reactor with the effective gas-liquid separator show a very different trend due to the surface aeration.

Taking all these aspects into account, in this paper, an equation was derived for the prediction of the downcomer gas holdup in airlift reactors in air-water systems, using available data from the literature and my experimental data. The downcomer gas holdup data in various types of airlift reactors are well represented by Eq. (7), with a respective correlation coefficient of 0.83. Eq. (7) predicts 137 data with a mean absolute percentage error of 21.1%.

$$\varepsilon_d = 1.85\varepsilon_r^{1.14}\left(\frac{A_d}{A_r}\right)^{0.284}\left(1+\frac{C_t}{L_d}\right)^{-1.92}\left(\frac{A_s}{A_r}\right)^{-0.652} - 0.216\left(\frac{L_{ch}}{L_d}\right)^{4.10}\left(\frac{A_b}{A_d}\right)^{6.25} \quad (7)$$

The ranges of the parameters are ε_d>0.01, $0.037 \le D_{ch}/L_d \le 0.638$, $0.108 \le A_d/A_r \le 4.928$, $0.170 \le A_s/A_r \le 4.858$, $1 \le (1+C_t/L_d) \le 1.367$, and $1.778 \le A_s/A_r \le 10.443$. It may be concluded that this correlation provides a reasonable estimation of the downcomer gas holdup in various types of airlift reactors.

The measured and calculated values of the downcomer gas holdup are given in Fig. 9. As already mentioned, the external-loop airlift reactor with the gas-liquid separator well-designed keeps the downcomer almost free of gas bubbles at lower gas velocity [77]. At higher gas velocity, either air pockets at the entrance of the downcomer or a vortex above it in the gas-liquid separator take place because of high circulation liquid velocity. The air pockets and the vortex accompany surface aeration [63]. The surface aeration hardly ever happens in other types of airlift reactors. However, despite the surface aeration, the downcomer gas holdup for the external-loop airlift reactor with the gas-liquid separator is much lower than that for other types of airlift reactors due to the effective gas-liquid separation. Therefore, the measured downcomer gas holdup in this study on average is approximately 53% lower than predicted by Eq. (7). It means that Eq. (7) maybe is not enough to describe the effect of the surface aeration on the downcomer gas holdup. We need further research to reflect well the surface aeration in a generally applicable equation for airlift reactor design.

We can use the correlations presented in this study for airlift reactor design. Eq. (5) and Eq. (7) allow us to gain various combinations of the operational and geometric parameters to obtain specific gas holdups. In particular, it will help determine one of the operational and geometric parameters, given all other parameters. The type of the reactor can be naturally determined from values of D_{ch}/L_d and A_s/A_r.

CONCLUSION

Most researchers have correlated their own data of gas holdup with the operational and geometric parameters for a particular type of airlift reactors. There was little attempt to obtain an equation that could correlate available gas holdup data, especially measured in different types of airlift reactors.

The geometric characteristics of airlift reactors exert an important influence on the riser and downcomer gas holdup. To successfully consider the geometric difference between various types of airlift reactors, the characteristic distance (D_{ch}) and the gas separation area (A_s) were defined and used in this work. The ratio of the characteristic distance to the downcomer length (D_{ch}/L_d) was found to be an effective parameter that could correlate many gas holdup data obtained in various types of airlift reactors, as was the ratio of the gas separation area to riser area (A_s/A_r).

A meaningful correlation involving U_{Gr} and dimensionless form of geometric parameters, such as $(1+C_t/L_d)$, D_{ch}/L_d, A_d/A_r, A_b/A_d,

A_s/A_r, was obtained for predicting the riser gas holdup in various types of airlift reactors. The downcomer gas holdup in various types of airlift reactors was well correlated by a nonlinear equation involving ε_r, $(1+C_t/L_d)$, D_{ch}/L_d, A_d/A_r, A_b/A_d, and A_s/A_r. Eq. (5) and Eq. (7) obtained in this study can be used in determining the type and dimensions of an airlift reactor.

It is a big step forward in generalization that we were able to represent a large amount of data from many researchers with one correlation at this time. Obtaining a correlation equation that can successfully represent much data on gas holdup obtained in various types of airlift reactors and air-water systems is the basis for deriving a more generalized correlation equation, reflecting the riser superficial liquid velocity, design of the gas sparger, and the properties of the liquid. To obtain a generalization that includes all other parameters that were not considered in this study, it will require the efforts of many researchers in the future.

NOMENCLATURE

A : cross-sectional area [m^2]
a : constant
b : constant
C_1 : constant=$\frac{3n+1}{n+1}$
C_2 : constant
C_b : bottom clearance [m]
C_s : dry weight solids per volume of suspension [%]
C_t : top clearance [m]
D : diameter [m]
D_{ch} : characteristic distance [m]
Fr′ : Froude number=$U_{Gr}^2/(g\phi)$
g : gravitational acceleration [m s^{-2}]
h : piezometer reading [m]
H : height [m]
H_d : aerated liquid height [m]
H_L : unaerated liquid height [m]
k : consistency index in a power-law model [Pa s^n]
L : length [m]
L_c : length of connection pipe [m]
L_h : distance between connection pipe axes [m]
M : Morton number=$g\mu_L^4/(\rho_L\sigma^3)$
n : flow index in a power-law model
P_G/V_L : power input per volume of degassed liquid [kw m^{-3}]
S : separator to downcomer volume ratio
T_{VR} : volume ratio
t_d : thickness of draft tube [m]
V_L : liquid volume [m^3]
V_{Lr} : mean liquid velocity in riser [m s^{-1}]
U_{Gr} : superficial gas velocity in riser [m s^{-1}]
U_{Lr} : superficial liquid velocity in riser [m s^{-1}]
W : width [m]
Z : height of pressure tap [m]

Greek Letters

ε : gas holdup
ν_g : kinematic gas viscosity [Pa s]
ν_{N_2} : kinematic nitrogen viscosity [Pa s]
μ : viscosity [Pa s]
μ_{eff} : effective viscosity [Pa s]
ρ : density [kg m^{-3}]
σ : surface tension [N m^{-1}]
ϕ : orifice size [m]

Subscripts

c : column
co : for L_c=0.50 m
d : downcomer or draft tube or vertical baffle
G : gas
L : liquid
r : riser
s : gas-liquid separator or gas separation
W : water

REFERENCES

1. P. Weiland and U. Onken, *Ger. Chem. Eng.*, **4**, 174 (1981).
2. M. Y. Chisti and M. Moo-Young, *Chem. Eng. Commun.*, **60**, 195 (1987).
3. J. C. Merchuk and H. Siegel, *J. Chem. Tech. Biotechnol.*, **41**, 105 (1988).
4. X. Lu, J. Ding, Y. Wang and J. Shi, *Chem. Eng. Sci.*, **55**, 2257 (2000).
5. C. H. Lin, B. S. Fang, C. S. Wu, H. Y. Fang, T. F. Kuo and C. Y. Hu, *Biotechnol. Bioeng.*, **18**, 1557 (1976).
6. T. Vorpongsathorn, P. Wongsuchoyo and P. Pavasnat, *Chem. Eng. J.*, **84**, 551 (2001).
7. K. H. Choi, J. W. Kim and W. K. Lee, *Korean J. Chem. Eng.*, **3**, 127 (1986).
8. M. Zhao, K. Niranjan and J. F. Davidson, *Chem. Eng. Sci.*, **49**, 2359 (1994).
9. S. Krichnavaruk and P. Pavasant, *Chem. Eng. J.*, **89**, 203 (2002).
10. L. Luo, J. Yuan, P. Xie, J. Sun and W. Guo, *Chem. Eng. Res. Des.*, **91**, 2377 (2013).
11. K. Mohanty, D. Das and M. N. Biswas, *Chem. Eng. Sci.*, **61**, 4617 (2006).
12. Y. Chisti, M. Kasper and M. Moo-Young, *Can. J. Chem. Eng.*, **68**, 45 (1990).
13. S. Goto and P. D. Gaspillo, *Chem. Eng. Sci.*, **13/14**, 3533 (1992).
14. T. Zhang, J. Wang, T. Wang, J. Lin and Y. Jin, *Chem. Eng. Proc.*, **44**, 81 (2005).
15. Y. Chisti and U. J. Jauregui-Haza, *Biotechnol. Eng. J.*, **10**, 143 (2002).
16. N. Lj. Lukić, I. M. Šijački, P. S. Kojić, S. S. Popović and M. N. Tokić, *Biochem. Eng. J.*, **118** 53 (2017).
17. H. Nikahtari and G. A. Hill, *Biochem. Eng. J.*, **27**, 138 (2005).
18. A. Margaritis and J. D. Sheppard, *Biotechnol. Bioeng.*, **23**, 2117 (1981).
19. H. Kawasaki, H. Hirano and H. Tanaka, *J. Chem. Eng. Japan*, **27**, 669 (1994).
20. J. C. Merchuk and H. Siegel, *AIChE J.*, **32**, 1585 (1986).
21. N. H. Thomas and D. A. Janes, *Fluid dynamic considerations in airlift bioreactors, in biotechnology processes scale-up and mixing*, C. S. Ho, J. Y. Oldshue (Eds.), AIChE, New York (1987).
22. J. C. Merchuk, N. Ladwa, A. Cameron, M. Bulmer, I. Berzin and M. Pickett, *AIChE J.*, **40** 1105 (1994).

23. M. Siegel and J. C. Merchuk, *Can. J. Chem. Eng.*, **69**, 465 (1991).
24. M. Blažey, G. M. Cartland Glover, S. C. Generalis and J. Markoš, *Chem. Eng. Pro.*, **43**, 137 (2004).
25. R. S. Douek, A. G. Livingston and G. F. Hewitt, *AIChE J.*, **41**, 2508 (1995).
26. Y. Kawase and N. Hashimoto, *J. Chem. Tech. Biotechnol.*, **65**, 325 (1996).
27. J. Lin, M. Han, T. Wang, T. Zhang, T. Wang and Y. Jin, *Chem. Eng. J.*, **102**, 51 (2004).
28. Y. Rujiruttanakul and P. Pavasant, *Chem. Eng. Res. Des.*, **89**, 2254 (2011).
29. S. H. Isaacs and M. Thoma, *Chem. Eng. Sci.*, **47**, 943 (1992).
30. B. Kochbeck, M. Lindert and D. C. Hempel, *Chem. Eng. Sci.*, **47**, 3443 (1992).
31. J. B. Snape, J. Zahradnik, M. Fialova and N. H. Thomas, *Chem. Eng. Sci.*, **50**, 3175 (1995).
32. C. Vail, E. Camarasa, S. Poncin, G. Wild, N. Midoux and J. Bouillard, *Chem. Eng. Sci.*, **55** 2957 (2000).
33. C. Vial, S. Poncin, G. Wild and N. Midoux, *Chem. Eng. Sci.*, **57**, 4745 (2002).
34. M. E. Orazem and L. E. Erickson, *Biothenol. Bioeng.*, **19**, 69 (1979).
35. W. Yu, T. Wang, M. Liu and Z. Wang, *Chem. Eng. J.*, **142**, 301 (2008).
36. T. Zhang, C. Wei, C. Feng and J. Zhu, *Bioresour. Technol.*, **104**, 600 (2012).
37. R. Salehpour, E. Jalilnejad, M. Nalband and K. Ghasemzadeh, *Particuology*, **51**, 91 (2020).
38. R. Bello, C. W. Robinson and M. Moo-Young, *Chem. Eng. Sci.*, **40**, 53 (1985).
39. K. Koide, K. Kurematsu, S. Iwamoto, Y. Iwata and K. Horibe, *J. Chem. Eng. Japan*, **16**, 413 (1983).
40. K. H. Choi, *Chem. Eng. Comm.*, **189**, 25 (2002).
41. E. R. Gouveia, C. O. Hokka and A. C. Badino-Jr., *Braz. J. Chem. Eng.*, **20**, 363 (2003).
42. M. Chakravarty, H. D. Singh, J. N. Baruah and M. S. Iyengar, *Ind. Eng. Chem.*, **16**, 17 (1974).
43. M. Y. Chisti, K. Fujimoto and M. Moo-Young, Paper 117a presented at AIChE Annual Meeting, Miami Beach, November 2-7 (1986).
44. R. A. Bello, C. W. Robinson and M. Moo-Young, *Can. J. Chem. Eng.*, **62**, 573 (1984).
45. Y. Kawase and M. Moo-Young, *J. Chem. Tech. Biotechnol.*, **36**, 527 (1986).
46. M. K. Popović and C. W. Robinson, *AIChE J.*, **35**, 393 (1989).
47. K. H. Choi and W. K. Lee, *J. Chem. Tech. Biotechnol.*, **56**, 51 (1993).
48. K. H. Choi, *Korean J. Chem. Eng.*, **18**, 240 (2001).
49. K. H. Choi, *Chem. Eng. Comm.*, **189**, 25 (2002).
50. F. Yazdian, S. A. Sojaosadati, M. Nosrati, M. Pesaran Hajiabbas and E. Vasheghani-Farahani, *Chem. Eng. Sci.*, **64**, 2455 (2009).
51. J. H. Hills, *Chem. Eng. J.*, **12**, 89 (1976).
52. J. C. Merchuk and Y. Stein, *AIChE J.*, **27**, 377 (1981).
53. T. Miyahara, M. Hamaguchi, Y. Suketa and T. Takahashi, *Can. J. Chem. Eng.*, **64**, 718 (1986).
54. J. Philip, J. M. Proctor, K. Niranjan and J. F. Davidson, *Chem. Eng. Sci.*, **45**, 651 (1990).
55. Z. Kemblowski, J. Przywarski and A. Diab, *Chem. Eng. Sci.*, **48**, 4023 (1993).
56. K. H. Choi, B. H. Han and W. K. Lee, *HWAHAK KONGHAK*, **28**, 220 (1990).
57. P. S. Kojić, M. S. Tokić, I. M. Šijački, N. Lj. Lukić, D. Lj. Petrović, D. Z. Jovičević and S. S. Popović, *Chem. Eng. Technol.*, **38**, 701 (2015).
58. L. Luo, F. Liu, Y. Xu and J. Yuan, *Chem. Eng. J.*, **175**, 494 (2011).
59. I. M. Šijački, M. S. Tokić, P. S. Kojić, D. Lj. Petrović, M. N. Tekić, M. S. Djurić and S. S. Milovančev, *Ind. Eng. Chem. Res.*, **50**, 6 (2011).
60. M. L. Fakhari, M. K. Moraveji and R. Davarnejad, *Chinese J. Chem. Eng.*, **22**, 267 (2014).
61. M. H. Siegel, J. C. Merchuk and K. Schugerl, *AIChE J.*, **32**, 1585 (1986).
62. P. S. Kojić, S. S. Popović, M. S. Tokić, I. M. Šijački, N. Lj. Lukić, D. Z. Jovičević and D. Lj. Petrović, *Braz. J. Chem. Eng.*, **34**, 493 (2017).
63. K. H. Choi, *Korean Chem. Eng. Res.*, **58**, 665 (2020).
64. R. Bello, C. W. Robinson and M. Moo-Young, *Biotechnol. Bioeng.*, **27**, 369 (1985).
65. C. Bentifraouine, C. Xuereb and J. P. Riba, *J. Chem. Tech. Biotechnol.*, **69**, 345 (1997).
66. A. Couvert, M. Roustan and P. Chatellier, *Chem. Eng. Sci.*, **54**, 5245 (1999).
67. W. A. Al-Masry, *Chem. Eng. Res. Des.*, **84**, 483 (2006).
68. A. G. Jones, *Chem. Eng. Sci.*, **40**, 449 (1985).
69. S. Wachi, A. G. Jones and T. P. Elson, *Chem. Eng. Sci.*, **46**, 657 (1991).
70. D. Lj. Petrović, D. Pošarac, A. Duduković and D. Skala, *J. Serb. Chem. Soc.*, **56**, 227 (1991).
71. W. J. Lu and S. J. Hwang, *Chem. Eng. Sci.*, **50**, 1301 (1995).
72. M. Blažey, M. Kiša and J. Markoš, *Chem. Eng. Pro.*, **43**, 1519 (2004).
73. M. Popović and C. W. Robinson, *Chem. Eng. Sci.*, **42**, 2811 (1987).
74. W. A. Al-Masry and A. R. Dukkan, *Chem. Eng. J.*, **65**, 263 (1997).
75. C. Bentifraouine, C. Xuereb and J. P. Riba, *Chem. Eng. J.*, **66**, 91 (1997).
76. M. Y. Chisti, B. Halard and M. Moo-Young, *Chem. Eng. Sci.*, **43**, 451 (1988).
77. Y. Chisti and M. Moo-Yong, *Chem. Eng. Pro.*, **9**, 38 (1993).
78. Y. Chisti, *Airlift bioreactors*, Elsevier Applied Science, London (1989).
79. K. H. Choi, Y. Chisti and M. Moo-Young, *Chem. Eng. J.*, **62**, 223 (1996).